

## Nitride tuning of lanthanide chromites

Ashley P. Black, Hannah Johnston, Judith Oró-Solé, Bernat Bozzo, Clemens Ritter, Carlos Frontera, J.Paul Attfield and Amparo Fuertes

### Supplementary Information

#### Experimental Details

The oxynitrides  $\text{RCrO}_{3-x}\text{N}_x$  ( $R = \text{La, Pr, Nd}$ ) were prepared by treatment under  $\text{NH}_3(\text{g})$  flow of  $600 \text{ cm}^3/\text{min}$  (Carbueros Metálicos, 99.9%) of  $\text{RCrO}_4$  precursor oxides between  $700$  and  $800 \text{ }^\circ\text{C}$ , using several cycles of  $10 \text{ h}$  with intermediate regrinding. The  $\text{RCrO}_4$  compounds were prepared using the Pechini method.  $\text{La}_2\text{O}_3$  (Aldrich, 99.9 %),  $\text{Pr}_6\text{O}_{11}$  (Aldrich, 99.9 %) or  $\text{Nd}_2\text{O}_3$  (Aldrich, 99.9 %) were first fired at  $900 \text{ }^\circ\text{C}$  during  $12 \text{ hours}$  and dissolved in  $\text{HNO}_3$   $0.1 \text{ M}$ . Then  $\text{Cr}(\text{NO}_3)_3 \cdot 9\text{H}_2\text{O}$  (Aldrich 99.99 %),  $\text{C}_6\text{H}_8\text{O}_7$  (citric acid, Aldrich 99.5 %) and  $\text{C}_2\text{H}_6\text{O}_2$  (ethylene glycol), were subsequently added to the solution in molar ratios  $R:\text{Cr}:\text{C}_6\text{H}_8\text{O}_7:\text{C}_2\text{H}_6\text{O}_2=1:1:1:1$ , with continuous stirring and heating at  $55\text{--}80 \text{ }^\circ\text{C}$ . The solutions were evaporated for  $12 \text{ h}$  to form the precursor resins that were subsequently treated in air at  $540 \text{ }^\circ\text{C}$  for  $15 \text{ hours}$ .

N contents were determined by combustion analysis in oxygen in a Thermo Fisher Scientific instrument, heating the samples in oxygen up to  $1060 \text{ }^\circ\text{C}$  and using  $\text{MgO}$ ,  $\text{WO}_3$  and  $\text{Sn}$  as additives and atropine as a reference standard.

X-ray powder diffraction data were collected on a Siemens D5000 diffractometer using  $\text{Cu K}\alpha$  radiation ( $\lambda = 1.5418 \text{ \AA}$ ). Synchrotron X-ray powder diffraction data at room temperature were measured from capillary ( $0.3 \text{ mm}$  diameter) samples in the angular range  $1.038^\circ \leq 2\theta \leq 61.09^\circ$  at the MSPD beamline<sup>1</sup> of the ALBA Synchrotron (Cerdanyola del Vallès, Spain). Using a double Si (111) crystal monochromator, a short wavelength was selected and calibrated with Si NIST ( $\lambda = 0.619714 \text{ \AA}$ ). Rietveld analysis was carried out using the program Fullprof.<sup>2</sup> Background refinement was performed by linear interpolation and the data were corrected for absorption.

Room temperature neutron powder diffraction data for  $\text{LaCrO}_{2.72}\text{N}_{0.28}$  was collected on the D2B diffractometer at the Institut Laue-Langevin (ILL), Grenoble using  $450 \text{ mg}$  of sample placed in a  $5 \text{ mm}$  diameter vanadium can. The neutron wavelength was  $1.594 \text{ \AA}$ . Room temperature data was collected for  $\text{NdCrO}_{2.58}\text{N}_{0.42}$  and  $\text{PrCrO}_{2.64}\text{N}_{0.36}$  on the D20 diffractometer also at the Institut Laue-Langevin. The neutron wavelength was  $1.36 \text{ \AA}$  using a take-off angle of  $118^\circ$ . Low temperature neutron powder diffraction was carried out on all the samples on D1B diffractometer at the ILL. The neutron wavelength was  $2.524 \text{ \AA}$ . For the  $R = \text{La}$  and  $\text{Nd}$  samples a series of scans were taken at intervals of approximately  $6.5 \text{ K}$  between  $10 \text{ K} - 315 \text{ K}$  for  $R = \text{La}$  and approximately  $3.5 \text{ K}$  between  $1.5 \text{ K} - 215 \text{ K}$  for  $R = \text{Nd}$ . For  $R = \text{Pr}$ , data was collected in  $50 \text{ K}$  intervals between  $1.5 \text{ K}$  and  $250 \text{ K}$ . Powder diffraction data were analysed using the FullProf software package.<sup>2</sup> The anion composition of the oxynitrides was constrained by the chemically determined value.

Magnetic measurements were performed between at  $H=2000 \text{ G}$  between  $10 \text{ K}$  and  $400 \text{ K}$  using a Quantum Design SQUID magnetometer.

**Table S1.** Summary of the *Pbnm* model for  $\text{LaCrO}_{2.72}\text{N}_{0.28}$  refined against room temperature synchrotron X-ray powder diffraction data. Refined cell parameters:  $a=5.52201(4)$ ,  $b=5.48192(5)$ ,  $c=7.6573(7)$  Å.  $R_{wp} = 4.33\%$ ,  $\chi^2 = 8.21$  for 59 variables.

Atom	Site	x	y	z	$B_{\text{iso}}$ (Å <sup>2</sup> )
La	4c	0.9978(2)	0.01274(9)	1/4	0.715(6)
Cr	4b	1/2	0.0	0.0	0.344(8)
X1	4b	0.070(1)	0.493(1)	1/4	0.31(4)
X2	8d	0.727(1)	0.268(1)	0.0353(5)	0.31(4)
		<b>La-X1</b>	<b>La-X2</b>	<b>Cr-X1</b>	<b>Cr-X2</b>
<b>Bond length / Å</b>		2.391(6)	2.474(5) × 2	1.980(1) × 2	1.953(6) × 2
		2.660(6)	2.640(6) × 2		1.989(6) × 2
		2.879(6)	2.821(5) × 2		
		3.136(6)	3.096(5) × 2		
		<b>Cr-X1-Cr</b>	<b>Cr-X2-Cr</b>		
<b>Bond Angle / °</b>		157.45(5)	161.5(3)		

**Table S2.** Summary of the *Pbnm* model for  $\text{PrCrO}_{2.81}\text{N}_{0.19}$  refined against room temperature synchrotron X-ray powder diffraction data. Refined cell parameters:  $a= 5.45535(4)$ ,  $b= 5.49076(3)$ ,  $c= 7.72751(5)$  Å.  $R_{wp} = 3.24\%$ ,  $\chi^2 = 3.93$  for 55 variables.

Atom	Site	x	y	z	$B_{\text{iso}}$ (Å <sup>2</sup> )
Pr	4c	0.9932(1)	0.03577(4)	1/4	0.610(4)
Cr	4b	1/2	0.0	0.0	0.158(8)
X1	4b	0.0736(9)	0.4815(5)	1/4	0.25(6)
X2	8d	0.7147(7)	0.2939(6)	0.0388(5)	0.25(6)
		<b>Pr-X1</b>	<b>Pr-X2</b>	<b>Cr-X1</b>	<b>Cr-X2</b>
<b>Bond length / Å</b>		2.382(5)	2.390(4) × 2	1.976(1) × 2	1.948(4) × 2
		2.486(3)	2.642(4) × 2		2.016(3) × 2
		3.075(3)	2.705(4) × 2		
		3.107(5)	3.286(4) × 2		
		<b>Cr-X1-Cr</b>	<b>Cr-X2-Cr</b>		
<b>Bond Angle / °</b>		155.80(4)	155.0(2)		

**Table S3.** Summary of the *Pbnm* model for NdCrO<sub>2.58</sub>N<sub>0.42</sub> refined against room temperature synchrotron X-ray powder diffraction data. Refined cell parameters: a=5.42787(3), b=5.50102(3), c=7.70936(4) Å.  $R_{wp} = 2.36\%$ ,  $\chi^2 = 7.72$  for 96 variables.

Atom	Site	x	y	z	B <sub>iso</sub> (Å <sup>2</sup> )
Nd	4c	0.9919(1)	0.04131(5)	1/4	0.787(7)
Cr	4b	1/2	0.0	0.0	0.17(1)
X1	4b	0.0851(9)	0.484(7)	1/4	0.53(4)
X2	8d	0.7190(7)	0.2935(7)	0.0410(5)	0.43(4)
		<b>Nd-X1</b>	<b>Nd-X2</b>	<b>Cr-X1</b>	<b>Cr-X2</b>
<b>Bond length / Å</b>		2.318(5)	2.401(4) × 2	1.984(1) × 2	1.928(4) × 2
		2.487(3)	2.591(4) × 2		2.030(4) × 2
		3.108(3)	2.716 (4) × 2		
		3.148(5)	3.300 (4) × 2		
		<b>Cr-X1-Cr</b>	<b>Cr-X2-Cr</b>		
<b>Bond Angle / °</b>		152.57(5)	155.0(2)		

**Table S4.** Summary of the *Pbnm* model for LaCrO<sub>2.72</sub>N<sub>0.28</sub> refined against room temperature neutron powder diffraction data. Refined cell parameters: a=5.5237(2), b=5.4787(2), c=7.7684(2) Å.  $R_{wp} = 2.45\%$ ,  $\chi^2 = 1.89$  for 41 variables.

Atom	Site	x	y	z	B <sub>iso</sub> (Å <sup>2</sup> )
La	4c	0.0037(8)	0.0152(7)	1/4	0.038(4)
Cr	4b	1/2	0.0	0.0	0.036(5)
X1	4b	0.0671(7)	0.487(1)	1/4	0.732(4)
X2	8d	0.7325(7)	0.2705(7)	0.0362(3)	0.732(4)
		<b>La-X1</b>	<b>La-X2</b>	<b>Cr-X1</b>	<b>Cr-X2</b>
<b>Bond length / Å</b>		2.376(6)	2.502(4) × 2	1.978(8) × 2	1.961(4) × 2
		2.613(8)	2.638(5) × 2		1.981(4) × 2
		2.911(8)	2.814(4) × 2		
		3.156(6)	3.085(4) × 2		
		<b>Cr-X1-Cr</b>	<b>Cr-X2-Cr</b>		
<b>Bond Angle / °</b>		158.05(3)	161.5(2)		

**Table S5.** Summary of the *Pbnm* model for PrCrO<sub>2.64</sub>N<sub>0.36</sub> refined against room temperature neutron powder diffraction data. Refined cell parameters: a= 5.3976(2), b= 5.4336(2), c= 7.6461(3) Å.  $R_{wp} = 1.40\%$ ,  $\chi^2 = 1.82$  for 128 variables.

Atom	Site	x	y	z	B <sub>iso</sub> (Å <sup>2</sup> )
Pr	4c	0.9959(2)	0.0302(8)	1/4	0.341(7)
Cr	4b	1/2	0.0	0.0	0.599(4)
X1	4b	0.0756(9)	0.4843(7)	1/4	0.599(4)
X2	8d	0.7106(5)	0.2904(5)	0.0403(4)	0.599(4)
		<b>Pr-X1</b>	<b>Pr-X2</b>	<b>Cr-X1</b>	<b>Cr-X2</b>
<b>Bond length / Å</b>		2.326(1)	2.348(6) × 2	1.956(1) × 2	1.958(3) × 2
		2.504(6)	2.635(7) × 2		1.969(3) × 2
		2.997(6)	2.687(5) × 2		
		3.095(1)	3.236(6) × 2		
		<b>Cr-X1-Cr</b>	<b>Cr-X2-Cr</b>		
<b>Bond Angle / °</b>		155.4(4)	154.5(1)		

**Table S6.** Summary of the *Pbnm* model for NdCrO<sub>2.58</sub>N<sub>0.42</sub> refined against room temperature neutron powder diffraction data. Refined cell parameters: a=5.3715(2), b=5.4459(2), c=7.6316(2) Å.  $R_{wp} = 1.36\%$ ,  $\chi^2 = 2.07$  for 93 variables.

Atom	Site	x	y	z	B <sub>iso</sub> (Å <sup>2</sup> )
Nd	4c	0.9930(9)	0.0388(5)	1/4	0.182(3)
Cr	4b	1/2	0.0	0.0	0.182(3)
X1	4b	0.0796(8)	0.4800(7)	1/4	0.897(4)
X2	8d	0.7097(5)	0.2944(5)	0.0421(4)	0.897(4)
		<b>Nd-X1</b>	<b>Nd-X2</b>	<b>Cr-X1</b>	<b>Cr-X2</b>
<b>Bond length / Å</b>		2.319(6)	2.340(4) × 2	1.958(1) × 2	1.946(3) × 2
		2.447(5)	2.602(4) × 2		1.985(3) × 2
		3.078(5)	2.674(4) × 2		
		3.092(6)	3.288(4) × 2		
		<b>Cr-X1-Cr</b>	<b>Cr-X2-Cr</b>		
<b>Bond Angle / °</b>		153.99(4)	153.16(1)		

**Table S7.** Summary of the magnetic refinements for *Pbnm* models at base temperatures using D1B neutron diffraction data. Refined lattice parameters and ordered moments at Cr and Nd sites are shown.

Sample	T/K	a/Å	b/Å	c/Å	$\mu_y(\text{Cr})/\mu_B$	$\mu_z(\text{Ln})/\mu_B$
LaCrO <sub>2.72</sub> N <sub>0.28</sub>	10	5.4508(9)	5.4086(6)	7.666(2)	2.73(5)	
PrCrO <sub>2.64</sub> N <sub>0.36</sub>	1.5	5.3258(7)	5.4039(7)	7.575(1)	2.60(8)	
NdCrO <sub>2.58</sub> N <sub>0.42</sub>	1.5	5.3569(7)	5.3922(6)	7.598(1)	2.59(5)	1.4(1)

**Table S8** Values of Curie temperatures and other magnetic parameters from Curie-Weiss fits to data above  $T_C$  for Ln = Pr and Nd samples (this was not possible for Ln = La due to the high  $T_C$ ). Effective Cr paramagnetic moments were estimated by subtracting the ideal Ln<sup>3+</sup> contribution from the total as shown in the Table footnote.

Ln, x <sup>[a]</sup>	$T_C$ /K	$T_{SR}$ /K	$\theta$ /K	$\mu_{\text{eff}}/\mu_B$	$\mu_{\text{eff}}(\text{Cr})/\mu_B$ <sup>[a]</sup>
La, 0	293				
La, 0.11	285				
La, 0.17	283				
La, 0.21	283				
La, 0.25	280				
La, 0.28	281				
Pr, 0	240	-	-217	5.50	4.17
Pr, 0.19	229	-	-156	5.17	3.73
Pr, 0.36	232	-	-43	4.30	2.38
Nd, 0	226	28	-251	4.72	3.03
Nd, 0.35	210	44	-138	5.21	3.75
Nd, 0.59	214	-	-91	4.60	2.84

<sup>[a]</sup>  $\mu_{\text{eff}}(\text{Cr}) = [\mu_{\text{eff}}^2 - \mu_{\text{eff}}(\text{Ln}^{3+})^2]^{1/2}$  where  $\mu_{\text{eff}}(\text{Pr}^{3+}) = 3.58$  and  $\mu_{\text{eff}}(\text{Nd}^{3+}) = 3.62 \mu_B$ .

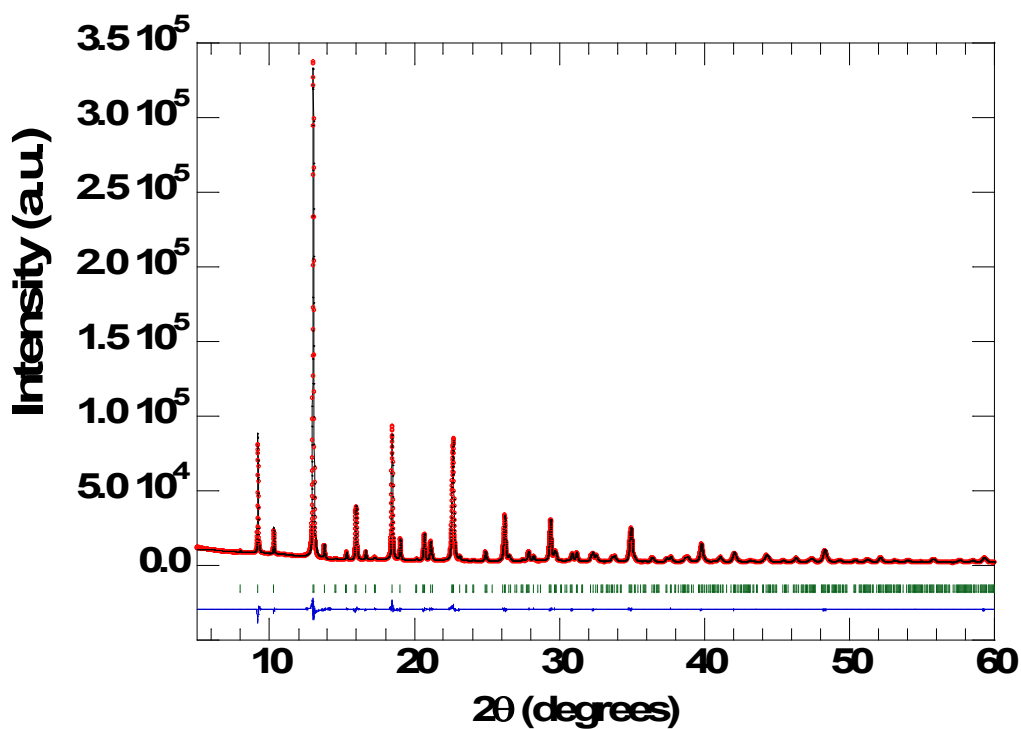


**Figure S1.** Observed and calculated synchrotron X-ray powder diffraction patterns for PrCrO<sub>2.81</sub>N<sub>0.19</sub>.

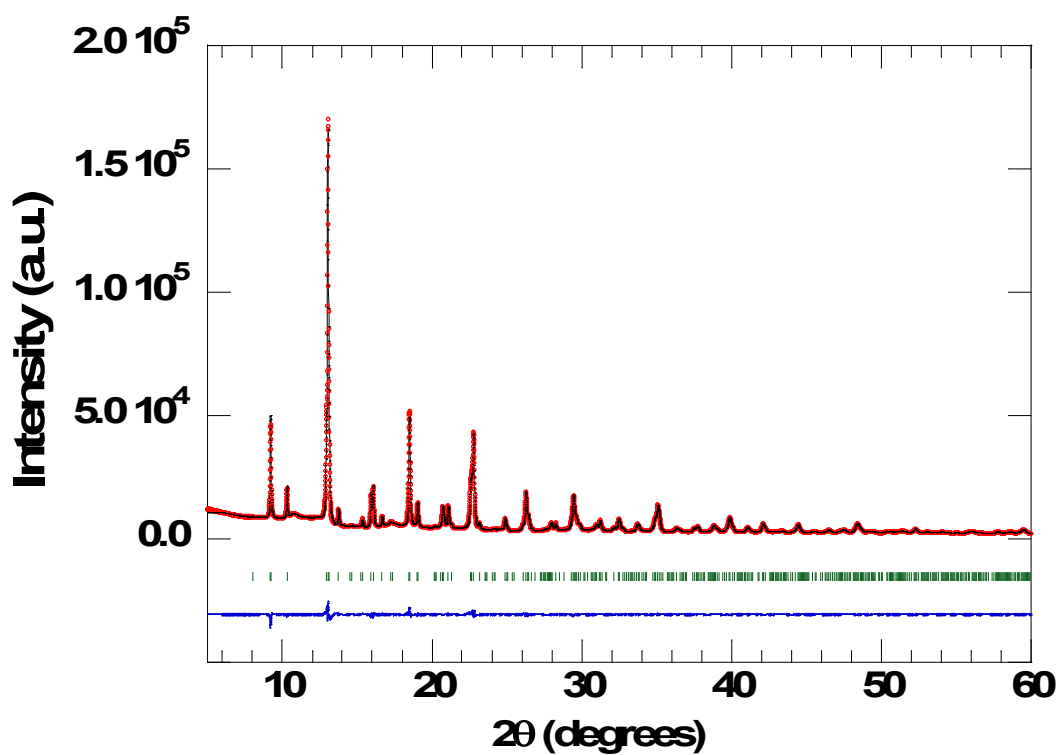


**Figure S2.** Observed and calculated synchrotron X-ray powder diffraction patterns for NdCrO<sub>2.58</sub>N<sub>0.42</sub>.

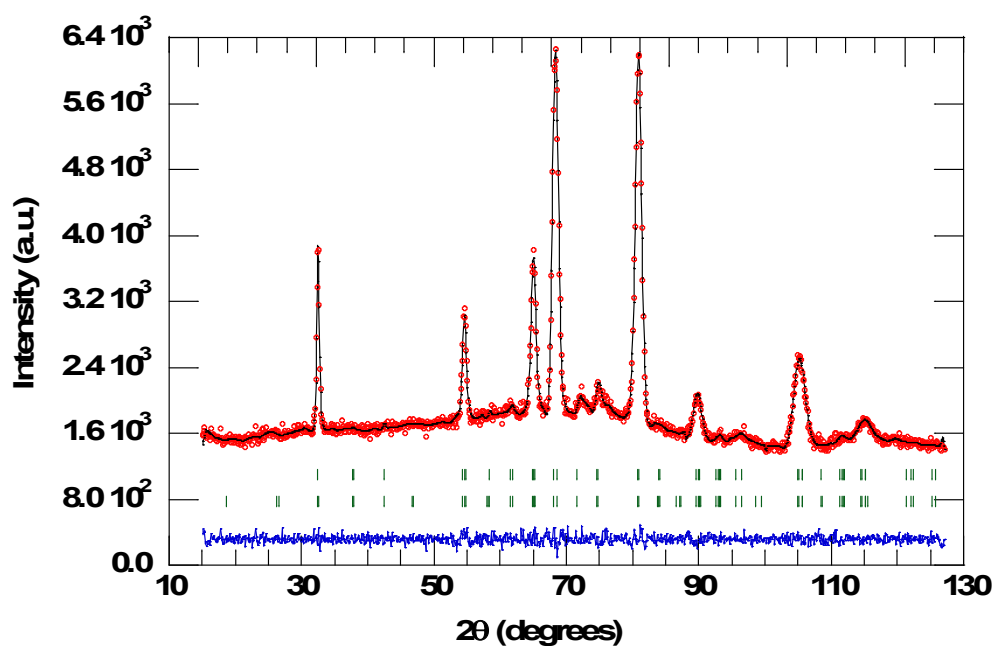


**Figure S3.** Observed and calculated 10 K neutron powder diffraction patterns for  $\text{LaCrO}_{2.72}\text{N}_{0.28}$  ( $\lambda=2.524 \text{ \AA}$ ).

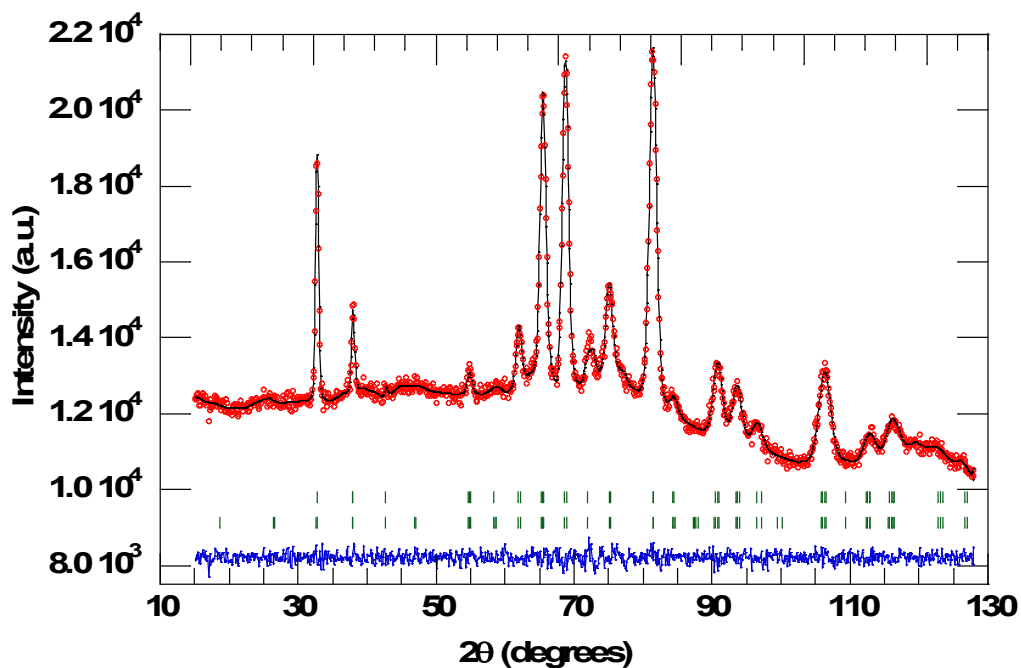


**Figure S4.** Observed and calculated 1.5 K neutron powder diffraction patterns for  $\text{PrCrO}_{2.64}\text{N}_{0.36}$  ( $\lambda=2.524 \text{ \AA}$ ).

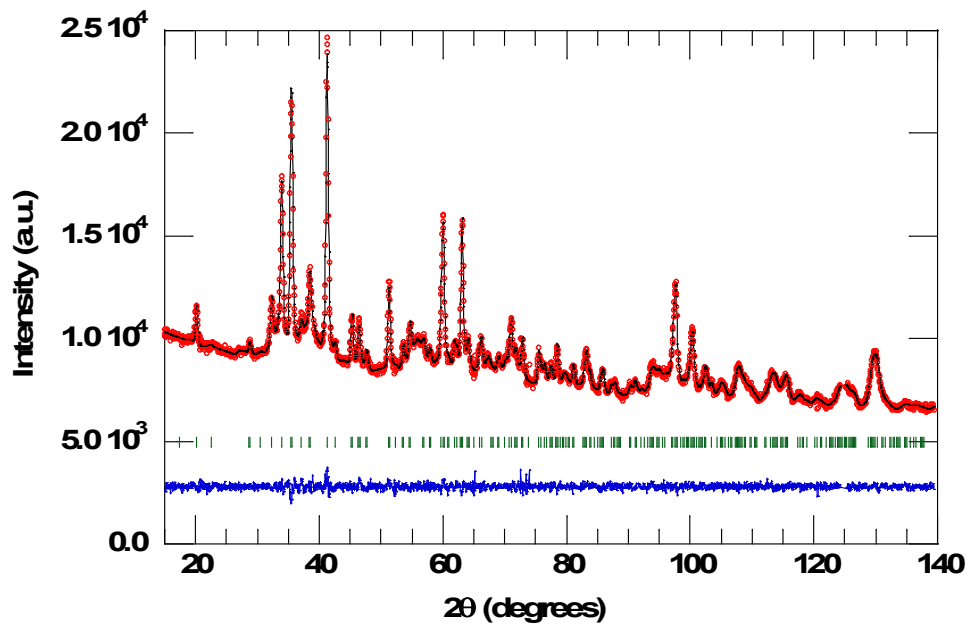


**Figure S5.** Observed and calculated room temperature neutron powder diffraction patterns for  $\text{PrCrO}_{2.64}\text{N}_{0.36}$  ( $\lambda = 1.36 \text{ \AA}$ )

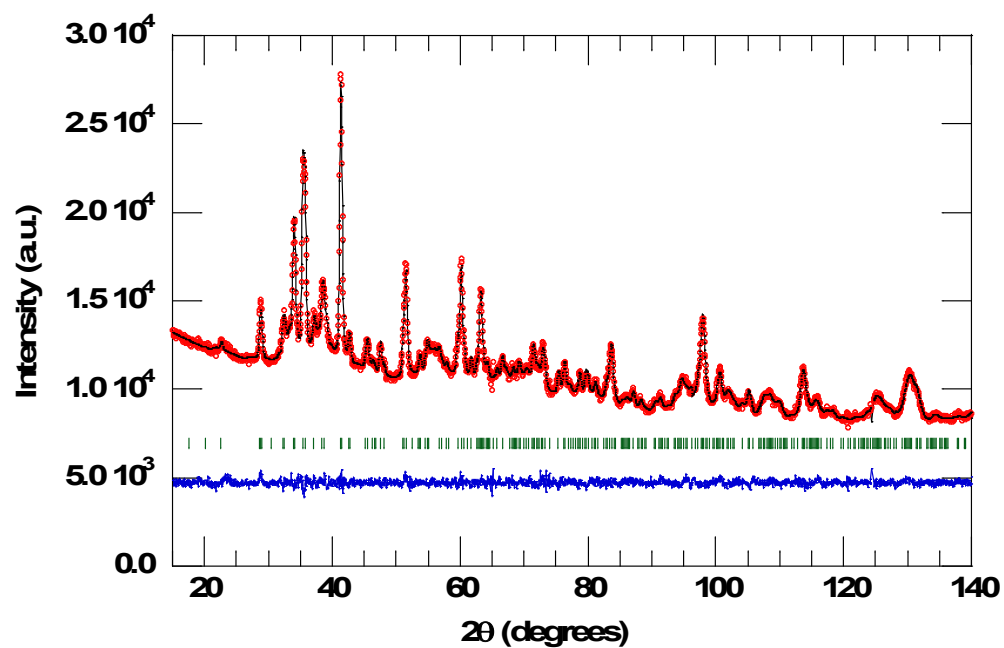


**Figure S6.** Observed and calculated room temperature neutron powder diffraction patterns for  $\text{NdCrO}_{2.58}\text{N}_{0.42}$  ( $\lambda = 1.36 \text{ \AA}$ ).



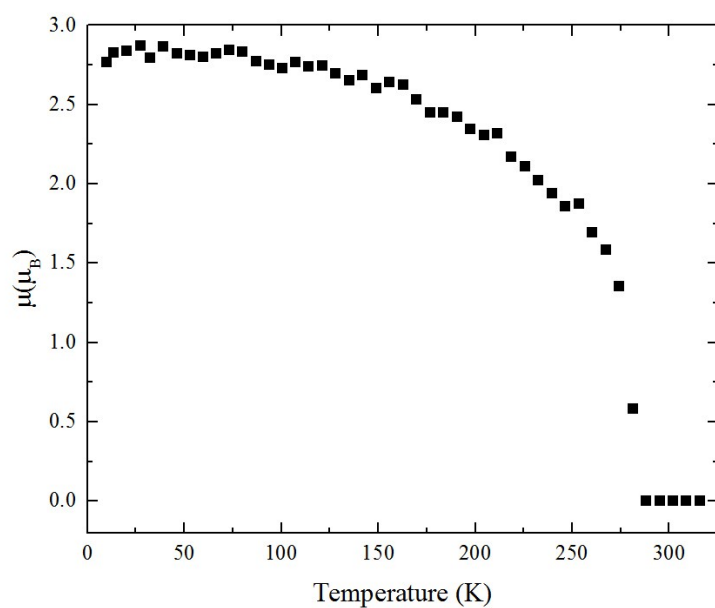


**Figure S7.** Thermal variation of refined Cr magnetic moment for  $\text{LaCrO}_{2.72}\text{N}_{0.28}$ .

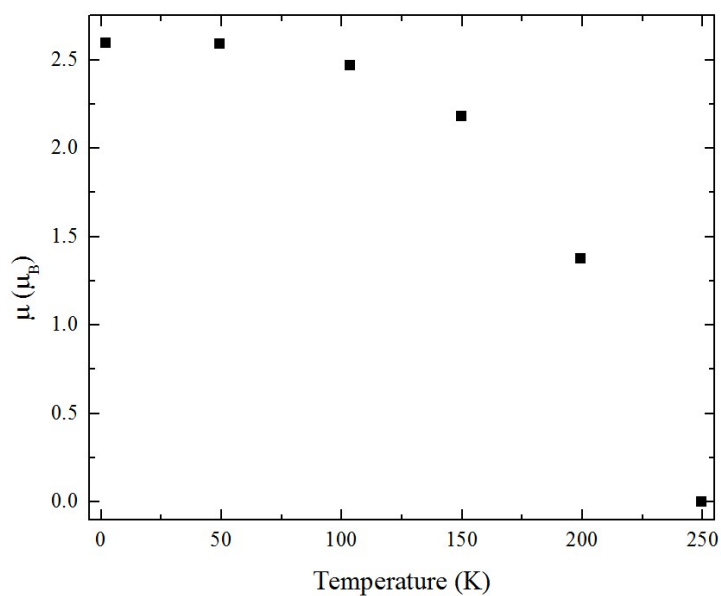


**Figure S8.** Thermal variation of refined Cr magnetic moment for  $\text{PrCrO}_{2.64}\text{N}_{0.36}$ .

<sup>1</sup> F. Fauth, I. Peral, C. Popescu, C. and M. Knapp, M. *Powder Diffraction* **28**, S360–S370 (2013).

<sup>2</sup> J. Rodríguez-Carvajal, *Phys. B*, 1993, **192**, 55.